

CROSSING THE TRANSCENDENTAL DIVIDE: FROM SCHOTTKY GROUPS TO ALGEBRAIC CURVES

SAMANTHA FAIRCHILD, ÁNGEL DAVID RÍOS ORTIZ

ABSTRACT. Though the uniformization theorem guarantees an equivalence of Riemann surfaces and smooth algebraic curves, moving between analytic and algebraic representations is inherently transcendental. Our analytic curves identify pairs of circles in the complex plane via free groups of Möbius transformations called Schottky groups. We construct a family of non-hyperelliptic surfaces of genus $g \geq 3$ where we know the Riemann surface as well as properties of the canonical embedding, including a nontrivial symmetry group and a real structure with the maximal number of connected components (an M -curve). We then numerically approximate the algebraic curve and Riemann matrices underlying our family of Riemann surfaces.

1. INTRODUCTION

Riemann surfaces are ubiquitous objects in mathematics. As such, they come in different incarnations such as geometric, analytic, and algebraic. Each incarnation has its advantages and is suitable for different purposes. Although the passage from the geometric to the algebraic side is theoretically possible, in order to make this passage effective (i.e. with a computer) we need to choose the right geometric and algebraic presentations. We give steps in bridging the *transcendental divide* between Riemann surfaces presented as quotients of Schottky groups, a presentation coming from Geometric Group Theory, and Riemann surfaces represented as canonical curves in CP^{g-1} , their most natural presentation in Algebraic Geometry.

Inspired by Bernd Sturmfels, and coined in [ÇFM22], the transcendental divide refers to the fact that explicitly or numerically connecting a Riemann surface to an algebraic curve requires transcendental functions, that is, functions which cannot be written as polynomials. The transcendental divide has been a large source of mathematics for the past century, inspired by work of Riemann, Poincaré, and Klein [FK92, Poi85]. A limiting aspect of working explicitly with the classical theory were the lack of computational tools, which have seen great advances in recent years [BK11]. Particular work includes computational work on computing Riemann theta functions [DHB⁺04], which has now been implemented in two programming languages [SD16, AC21].

We have three main contributions. Firstly, we construct an interesting family of non-hyperelliptic Riemann surfaces that admit an action of the dihedral group and their real structure attains the maximal number of ovals. Secondly, we present an algorithm that evaluates the canonical image of a Riemann surface given in terms of Schottky data. Finally, we show in low genus how our algorithm effectively captures the theoretical properties of our family of curves. This is showed in low genus by approximating the ideal of a curve and computing its Riemann matrix. One of the main features of our framework is its flexibility, paving the way of extending

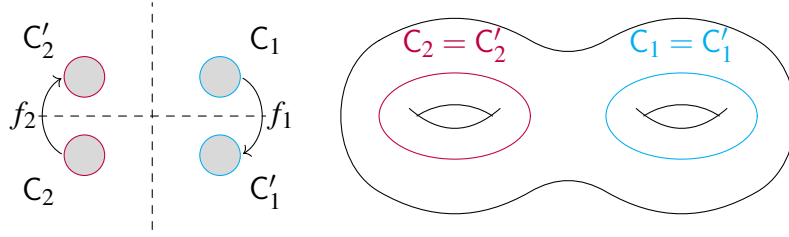


FIGURE 1. A genus 2 curve by gluing the circles C_j to C'_j for $j = 1, 2$ under Möbius transformations f_1, f_2 .

our work for higher genus and therein bringing together again Geometric Group Theory, Algebraic Geometry and Computational Mathematics. We now introduce some notation in order to describe our results.

We construct a genus $g \geq 2$ Riemann surface as follows. Given $2g$ circles C_1, \dots, C_g and C'_1, \dots, C'_g , where each pair of circles are disjoint circles in the Riemann sphere \mathbf{CP}^1 and C_j, C'_j have the same radius (See Fig. 1), consider Möbius transformations f_1, \dots, f_g which map the inside of C_j to the outside of C'_j for each $j = 1, \dots, g$. The (classical) Schottky group G is the free group generated by f_1, \dots, f_g . Each generator f_j has fixed points A_j, B_j , and the limit set Λ is the union of orbits of A_j, B_j for $j = 1, \dots, g$. The group G acts freely and properly discontinuously on the domain of discontinuity $\Omega = \mathbf{CP}^1 \setminus \Lambda$, and the genus g Riemann surface is given by the quotient Ω/G . The study of Schottky groups and other discrete subgroups of $\mathrm{PSL}(2, \mathbf{C})$ is a beautiful and rich theory, with some accessible entry points from [MSW02, Mar16].

The key transcendental functions in this paper are *Poincaré theta series* [Poi85, p. 148], which define a basis of Abelian differentials on the Riemann surface S .

Proposition 1.1. [BK11, Section 5.1] *The following Poincaré theta series, when convergent, form a basis of holomorphic differentials for $n = 1, \dots, g$*

$$\omega_n = \sum_{f \in G/G_n} \left(\frac{1}{z - f(B_n)} - \frac{1}{z - f(A_n)} \right) dz$$

where G/G_n are cosets with representatives given by all elements $f_{i_1}^{j_1} \cdots f_{i_k}^{j_k}$ where $i_k \neq n$ and A_n, B_n are the fixed points of f_n .

By evaluating these series we obtain the *canonical map* defined by

$$\phi_S : S \longrightarrow \mathbf{CP}^{g-1}; \quad z \mapsto [\omega_1(z) : \cdots : \omega_g(z)]. \quad (1.1)$$

The benefit of studying the canonical maps is that the *extrinsic* geometry of the Riemann surface in \mathbf{CP}^{g-1} is reflected in the *intrinsic* structure of the Riemann surface itself. For hyperelliptic Riemann surfaces, as is the case for genus two, the map ϕ_S is a $2 : 1$ map onto \mathbf{CP}^1 , whereas for *general* Riemann surfaces ϕ_S turns out to be an embedding.

1.1. A new family of examples. We are not aware of any explicit equations for a single canonical curve coming from a Schottky group, but we include after the statement of our results some context of different techniques used for understanding the canonical curve for Schottky groups

in general. The main result of this paper constructs a family of Schottky groups where the curves have a real structure and sufficiently many automorphisms to verify the computational efficacy of the approximate canonical curve. This theorem includes work of Hidalgo [Hid02] in the case of genus 3, and extends the family of examples to arbitrary genus.

We now present the construction of our family of examples and refer to Section 2.2 for the relevant notations. We denote $C(z_i, r)$ for the circle of radius r centered at z_i .

Definition 1.2. Fix a genus $g \geq 2$. Let $0 < \eta < \theta < \frac{\pi}{g}$ be real numbers. Define a Riemann surface $S_{\eta, \theta}$ constructed from a Schottky group $G_{\eta, \theta}$ defined by identifying the circle pairs from the curves $C_i = C(z_i, r)$ to $C'_i = C(w_i, r)$ with positive real trace where C_1 is the curve orthogonal to the unit circle passing through $e^{i\eta}$ and $e^{i\theta}$, C'_1 is the conjugate of C_1 , and the remaining C_i are given by rotations of $\frac{2\pi i}{g}$ (see Fig. 2 for $g = 3$).

To state the properties of $S_{\eta, \theta}$, we need the following definitions. A *real structure* on a Riemann surface X is an anti-holomorphic involution τ . A real surface X is called an *M-curve* if it attains the maximum number of ovals fixed under τ , namely $g + 1$. We will use the geometric convention that D_g represents the dihedral group of order $2g$. Recall that the signature of a group H acting holomorphically on a Riemann surface X is the tuple $(g_0; m_1, \dots, m_s)$ where g_0 is the genus of the quotient X/H and the map $X \rightarrow X/H$ is branched over s points with orders m_1, \dots, m_s .

Theorem 1.3. The Riemann surface $S := S_{\eta, \theta}$ is an M-curve with real structure defined by inversion about the unit circle $z \mapsto 1/\bar{z}$, which is invariant under the action of the Schottky group $G := G_{\eta, \theta}$. The group of automorphisms $\text{Aut}(S)$ contains the dihedral group D_g , which acts on S with signature $(0; 2, 2, 2, 2, g)$.

We have the following results split into the hyperelliptic case $g = 2$, and the non-hyperelliptic case $g \geq 3$. Recall that a Weierstrass point in a Riemann surface X is a point P for which there exists a meromorphic function with a single double pole at P .

Theorem 1.4. For $g = 2$, the Riemann surface $S_{\eta, \theta}$ is represented by $y^2 = \prod_{j=1}^6 (x - \tilde{\phi}_S(x_j))$, where the x_j are the Weierstrass points

$$x_1 = 1, \quad x_2 = -1, \quad x_3 = e^{i\theta}, \quad x_4 = e^{i\eta}, \quad x_5 = e^{i(\pi-\theta)}, \quad x_6 = e^{i(\pi-\eta)}$$

and $\tilde{\phi}(z) = \omega_2(z)/\omega_1(z)$ is the coordinate chart where $\omega_1(z) \neq 0$, and the images $\tilde{\phi}(x_j)$ are real and given in reciprocal pairs.

See Fig. 2 for reference of the Weierstrass points in Theorem 1.4.

Theorem 1.5. For $g \geq 3$, the Riemann surface $S := S_{\eta, \theta}$ is not hyperelliptic. Hence the canonical map $\phi_S : S \rightarrow \mathbf{CP}^{g-1}$ is an embedding.

In the case of low genus, we can use Theorem 1.5 to give the exact form of the curve in terms of fixed points of ϕ_S . In Section 4 we explore these symmetries for genus 3 and 4.

Riemann surfaces of the same genus can be grouped in a moduli space \mathcal{M}_g . Roughly speaking, the moduli space of genus g Riemann surface is a complex manifold with the property that

every family of Riemann surfaces of genus g has a unique map to \mathcal{M}_g . There are two ways of doing this: One analytical (mapping class groups) and one algebraic (stacks). See [ACG11] for more details. There are many interesting questions that arise from studying the geometry of the family of Riemann surfaces from Definition 1.2 that are beyond the scope of this paper, but we include a short discussion in Section 6.3 for those interested. We highlight that an important benefit of Definition 1.2 is that the range of values for θ and η provides a continuous, 2-dimensional, real parametrization for a family in \mathcal{M}_g .

1.2. Numerical approximations. In Section 5, we use Definition 1.2 as our test case to numerically evaluate the canonical map by taking finite approximations of the series. In genus 2 (Section 5.2) we approximate the Weierstrass points, which are the fixed points under the hyperelliptic involution. In genus ≥ 3 we will not work with hyperelliptic curves, and by sampling a distribution of points on S , approximate the equations of the algebraic curve (Section 5.3).

To do the numerical approximations, we give Algorithm 5.1 as a convenient source for those hoping to implement the techniques of these approximations for examples outside of the scope of this paper. Given a list of isometric circles, we construct Schottky group elements identifying the circles and construct the elements of the Schottky group of bounded word length. This uses classical properties of Möbius transformations and the Breadth First search presented in [MSW02, p.115] in updated language. The full code was implemented in Julia [BEKS17] and source code can be found in [Mat24].

In Section 5.4 we give the formula for approximating the Riemann matrix associated, and compute a specific example for genus 3. Recall a Riemann matrix is a $g \times g$ matrix with positive definite imaginary part. For M -curves, we can in fact always represent the Riemann matrix as a purely imaginary matrix. The power of M -curves arise in the study of solutions to the Kadomtsev–Petviashvili (KP) partial differential equation which is used to describe nonlinear wave motion. In fact M -curves are all of the nonsingular integrable (specifically finite-gap) solutions of the KP equation [Bob88]. In addition to the computational work surrounding

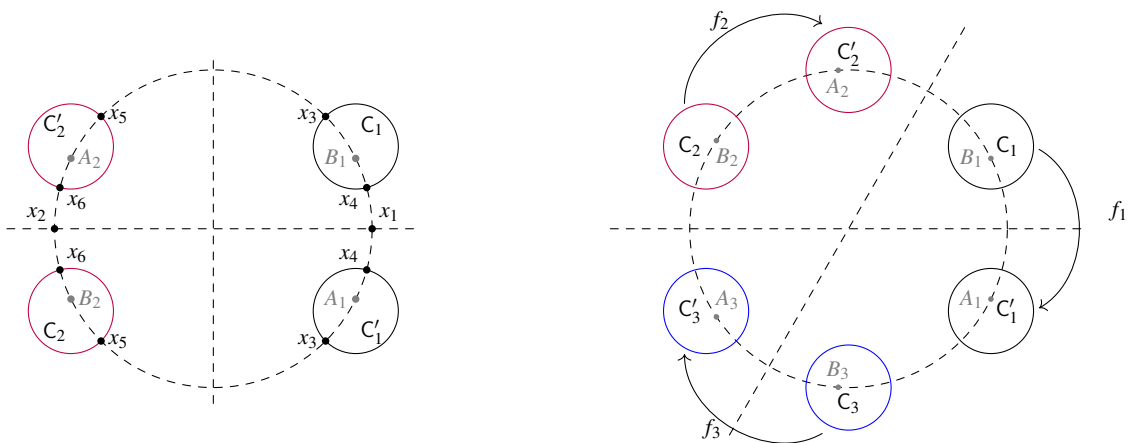


FIGURE 2. Examples of the curves from Definition 1.2 for $g = 2, 3$ on the left and right respectively with fixed points A_j and B_j the attracting (resp. repelling) fixed points of f_j . Also on the left see Theorem 1.4 for the Weierstrass points x_i .

M -curves contained in [BK11], see also more recent work on M -curves for example in mathematical physics [AG22] and algebraic geometry [KS22].

1.3. Connection to other works. When $g = 2$, a Riemann surface is always hyperelliptic, in which case the algorithms are not necessarily the most efficient. In the case of real hyperelliptic surfaces, there exist more efficient algorithms for evaluating the series in Proposition 1.1 due to S. Yu. Lyamaev [Lya22]. For those needing more efficient computations than those presented in this paper, we recommend beginning with extremal polynomials [Bog12]. There is a stronger version of hyperellipticity coming from hyperelliptic Schottky groups, where hyperelliptic structure of the curve can be seen in the group structure as well, see [Kee80] and more recently in [GK05].

Staying in the genus 2 setting, in [HF05], they provide an example where they solve the inverse uniformization theorem by (numerically) constructing a Schottky group that normalizes Bolza’s curve. In addition to being of independent interest for numerical results related to Schottky groups on genus 2 curves, the numerical results of [HF05] are particularly useful to provide calibration of our code. We remark however that in [HF05], they consider a slightly different series, and to calibrate our results, we can use the fact that our series match at -1 and $1/\sqrt{3}$ for $F_{\frac{\pi}{6}}$. Other examples within the hyperelliptic setting include a result on constructing Schottky groups and associated algebraic curves for any genus $g \geq 2$ for a family of hyperelliptic curves called May’s surfaces in [Hid02].

We refer the reader to [Hid05a] for more information on the study of automorphism groups for Schottky groups, and to [Hid05b, BHQ18, Hid24] for further discussions on the connections between Schottky groups and real structures in the hyperelliptic and non-hyperelliptic cases. We will focus on curves over \mathbf{C} , but there are rich analogous theories over other field. Over p -adics, one can also consider Schottky groups, for which the images are then called Mumford Curves [Mum72], see [GvdP80, Page 37] and the recent work of J. Poineau and D. Turchetti, see [PT21a, PT21b, PT22]. Over algebraic numbers, the theory of Dessins d’Enfants gives a way to construct such algebraic curves via Beyl’s theorem [JW16].

1.4. Outline. We begin the paper with Preliminaries in Section 2 covering the necessary background in Algebraic curves, Schottky groups, as well as necessary conditions for convergence of the series in Proposition 1.1. In Section 3 we prove the main theorems of the paper: Theorem 1.3, Theorem 1.4 and Theorem 1.5. In Section 4 we include the computations needed to obtain explicit algebraic curves, which are then used in the numerical experiments in Section 5. We conclude with some final remarks and future directions in Section 6.

Acknowledgements. The authors would like to thank Bernd Sturmfels for connecting us on this problem and Alex Elzenaar for contributions at the beginning of this project. We would also like to thank Benjamin Hollering and Türkü Ozlüm Çelik for useful discussions. Fairchild was partially supported by Deutsche Forschungsgemeinschaft (DFG) - Project number 507303619. Rios Ortiz was supported by the European Research Council (ERC) under the European Union’s Horizon 2020 research and innovation programme (ERC-2020-SyG-854361-HyperK).

2. PRELIMINARIES

In this section we provide some background and references for more detailed analysis on Algebraic curves (Section 2.1) and Schottky groups (Section 2.2).

2.1. From Riemann surfaces to algebraic curves. Every compact Riemann surface S can be embedded in the projective space \mathbf{CP}^n for large enough n as a complex *algebraic* submanifold. In other words, there exists a homogeneous ideal $I \subset \mathbf{C}[z_0, \dots, z_n]$ such that S is biholomorphic to the set of common zeroes of I in \mathbf{CP}^n .

Example 2.1. Any Riemann surface S of genus 1 can be embedded in \mathbf{CP}^2 as a plane cubic curve, that is the zero set of a homogeneous polynomial of degree 3 in the variables z_0, z_1, z_2 . After fixing a point they inherit a group law, these are also called elliptic curves.

Once we have an embedding of a Riemann surface S in \mathbf{CP}^n , if $n > 3$ we can always isomorphically project S onto \mathbf{CP}^{n-1} . This shows that every Riemann surface can be embedded as an algebraic submanifold of \mathbf{CP}^3 , cf. [GH78, pp. 215]. However, and this will be important later, we prefer embeddings that are *intrinsic*. In the following we will describe such embeddings.

Let S be a compact Riemann surface of genus g . The *canonical bundle* Ω_S of S is the dual of the holomorphic tangent bundle on S . Abelian differentials on S are global sections of Ω_S . Locally any Abelian differential can be written as $f(z)dz$, where $f(z)$ is a holomorphic function. Denote by $H^0(S, \Omega_S)$ the vector space of Abelian differentials on S , then a classical theorem due to Riemann states that $H^0(S, \Omega_S)$ has dimension g . Let $\omega_1, \omega_2, \dots, \omega_g$ be a basis of $H^0(S, \Omega_S)$. Pointwise evaluation induces the so-called *canonical map*:

$$\phi_S : S \dashrightarrow \mathbf{CP}^{g-1}, \quad z \mapsto [\omega_1(z) : \dots : \omega_g(z)]. \quad (2.1)$$

This map is unique up to a change of basis. Notice that in principle ϕ_S might not be defined everywhere, meaning that there could be points in S which are evaluated to zero for all elements in the basis, Theorem 2.3 below excludes that case and moreover, says that ϕ_S is an embedding if and only if there exists no meromorphic function on S having exactly two poles, this last condition means that S is *hyperelliptic*.

Definition 2.2. A compact Riemann surface S is called *hyperelliptic* if S can be expressed as a two-sheeted branched covering of \mathbf{CP}^1 . The induced covering involution on S is called the *hyperelliptic involution*.

Theorem 2.3. [FK92, III.10.2] Let S be a compact Riemann surface of genus $g > 1$, then the canonical map is defined everywhere. The canonical map is an embedding if and only if S is not hyperelliptic. The degree of S under the canonical map is $2g - 2$.

Remark 2.4. The canonical map characterizes non degenerate smooth complex Riemann surfaces of genus g and degree $2g - 2$ in \mathbf{CP}^{g-1} , see [FK92, pp.139].

To study the excluded case in Theorem 2.3, let $f : S \rightarrow \mathbf{CP}^1$ be a hyperelliptic Riemann surface. By the Riemann-Hurwitz formula [GH78, pp. 216] f has $2g + 2$ ramification points

(called *Weierstrass points*) and hence $2g + 2$ branch points z_1, \dots, z_{2g+2} in \mathbf{CP}^1 . Therefore S is the Riemann surface associated to the algebraic function

$$w^2 = (z - z_1) \cdots (z - z_{2g+2}). \quad (2.2)$$

With the representation given in 2.2 an explicit basis (see [GH78, pp. 253] or [FK92, III.10.3] for more details) for $H^0(S, \Omega_S)$ is given by the following differentials $\omega_1 = \frac{dz}{w}$, $\omega_2 = z \frac{dz}{w}$, \dots , $\omega_g = z^{g-1} \frac{dz}{w}$. The canonical map therefore factorizes in the following way

$$\begin{array}{ccc} S & \xrightarrow{\phi_S} & \mathbf{CP}^{g-1} \\ & \searrow f & \nearrow v_{g-1} \\ & & \mathbf{CP}^1 \end{array} \quad (2.3)$$

where v_{g-1} is the *Veronese embedding* of degree $g - 1$, namely the map given in projective coordinates by $v_{g-1}([z : w]) = [z^{g-1} : z^{g-2}w : \dots : w^{g-1}]$. Every Riemann surface of genus $g \leq 2$ is hyperelliptic. Representations of hyperelliptic Riemann surfaces can be made very explicit using Weierstrass models, that is equations of the form 2.2, see [FK92, VII.4] or [Bog12] for a more computational approach. Although our main interest in this work are non-hyperelliptic surfaces, we will deal with hyperelliptic curves in 1.4.

Starting from genus $g \geq 3$ the *general* Riemann surface is not hyperelliptic and therefore the canonical map is an embedding. We are interested in the *equations* defining this embedding. In genus 3 and 4 non-hyperelliptic Riemann surfaces will be *complete intersections*.

Lemma 2.5. [GH78, pp. 256-259] *Let S be a compact Riemann surface of genus g . Assume that S is not hyperelliptic so ϕ_S is an embedding. If $g = 3$, then the ideal $I_{\phi_S(S)}$ is generated by a unique polynomial of degree 4. If $g = 4$, then $I_{\phi_S(S)}$ is generated by two polynomials of degree 2 and 3 respectively.*

2.2. Geometry of Schottky groups. *Kleinian groups* are defined as discrete subgroups $G \leq \mathrm{PSL}(2, \mathbf{C}) = \mathrm{Aut}(\mathbf{CP}^1)$. In particular every Schottky group (see Introduction) is Kleinian. Recall, in Section 1 we defined the region $\Omega = \mathbf{CP}^1 \setminus \Lambda(G)$ to be the *domain of discontinuity*; where $\Lambda := \Lambda(G)$ is the limit set. Every Riemann surface of genus at least 2 can in fact be realized as a Kleinian group.

Theorem 2.6 (Kleinian uniformization). [Mas87, Section VIII.B] *Let S be a Riemann surface of genus at least 2. There exists a planar open set Ω and a group G of Möbius transforms which preserves Ω , such that S is biholomorphic to Ω/G .*

We refer the reader to Fig. 3 for a visualization of different limit sets for Schottky groups. One can generally construct Schottky groups by identifying pairs of isometric circles. On the left of Fig. 3 is the Fuchsian case, where all circles have centers on a common circle or line, plotted in the case of Definition 1.2 for $g = 2$, $\theta = \frac{5\pi}{12}$, $\eta = \frac{\pi}{12}$. In the middle is a classical Schottky group where the circles are disjoint but in more general positions. If the circles are allowed to overlap, there is still a notion of Schottky group, where the limit set becomes more interesting as shown in the right of Fig. 3.

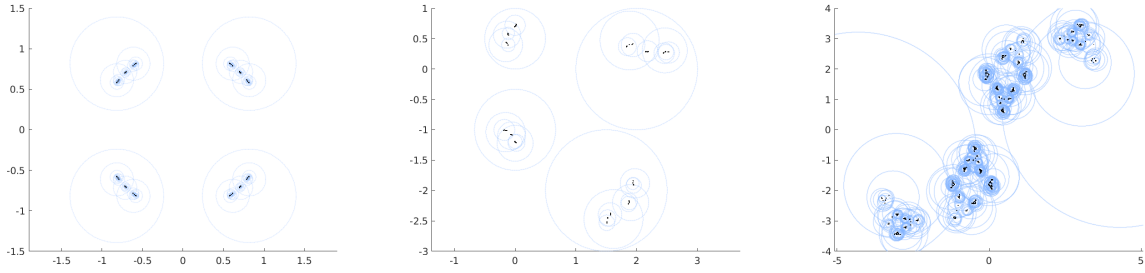


FIGURE 3. From left to right, three different limit sets Λ for Fuchsian, classical, and general Schottky groups of genus 2. We represent Λ in dark blue and the light blue circles are images of the isometric circles under the elements in G .

We now restrict ourselves to the case of Fuchsian Schottky groups introduced in Section 1. In this case the limit set is a discrete subgroup of the unit circle. This comes from the fact that the Schottky group leaves the unit circle unchanged so the fixed points, and all orbits of the fixed points reside on the circle. Such a group is called *Fuchsian*. In general the complement of $\Omega(G)$ can be rather wild as shown in Fig. 3. We have the following result which is a special case of the results stated in [Rat06, §12.2] or [Mas87, §II.G,IV.J].

Proposition 2.7. *Let G be a Schottky group with generators f_1, \dots, f_g pairing disjoint circles with disjoint interiors C_1, \dots, C_g with C'_1, \dots, C'_g so that $f_i(C_i) = C'_i$ and the image of the region bounded by C_i under f_i is the region outside of C'_i .*

- (1) G is free on f_1, \dots, f_g
- (2) G is discrete
- (3) The common exterior U defined to be the complement of the $2n$ regions bounded by the C_i, C'_i forms a fundamental domain for G .
- (4) Ω/G is a compact surface of genus g .

The proof requires the Poincaré Polyhedron theorem [Rat06, §11.2] or [Mar16, §IV.H], which we use in Proposition 3.1.

We conclude this section by discussing the series in Proposition 1.1. Their convergence is summarized in [Bog12, §6.1.2], by making use of the so-called *Schottky criterion*, which gives a sufficient condition for the series to converge absolutely and uniformly on compact subsets of Ω , see [Bog12, Bob88].

3. PROOF OF MAIN THEOREMS

In this section we will prove Theorem 1.3, Theorem 1.4 and Theorem 1.5. The idea is to generalize a construction by Hidalgo [Hid02, §6] in order to get a Fuchsian Schottky group with many symmetries. Fix an integer $g > 1$ and real numbers η, θ such that $0 < \eta < \theta < \pi/g$. Let $L \subset \mathbf{C}$ be the line of slope π/g through the origin and recall C_1 is the circle orthogonal to the unit circle $S^1 \subset \mathbf{C}$ through the points $e^{i\theta}$ and $e^{i\eta}$; these objects are shown in Fig. 2. Now define $\sigma, \sigma_1, \sigma_2$, and σ_3 to be respectively the reflections across S^1 , the real line $\mathbf{R} \subset \mathbf{C}$, L , and C_1 (see Fig. 4)

Construct two conformal mappings $r = \sigma_2 \circ \sigma_1$ and $h = \sigma \circ \sigma_1$; these are respectively the clockwise rotation about 0 by the angle $2\pi/g$ written as $z \mapsto e^{\frac{2\pi i}{g}} z$ and the order 2 automorphism with fixed points ± 1 given by $z \mapsto 1/z$.

For $k \in \mathbf{Z}$, define the element $f_k := r^k \circ \sigma_1 \circ \sigma_3 \circ r^{-k}$, and use these to generate the group

$$G := \langle f_k : 0 \leq k \leq g-1 \rangle.$$

Let $S := \Omega(G)/G$ be the Riemann surface of genus g obtained as a quotient. We can now prove the last part in 1.3.

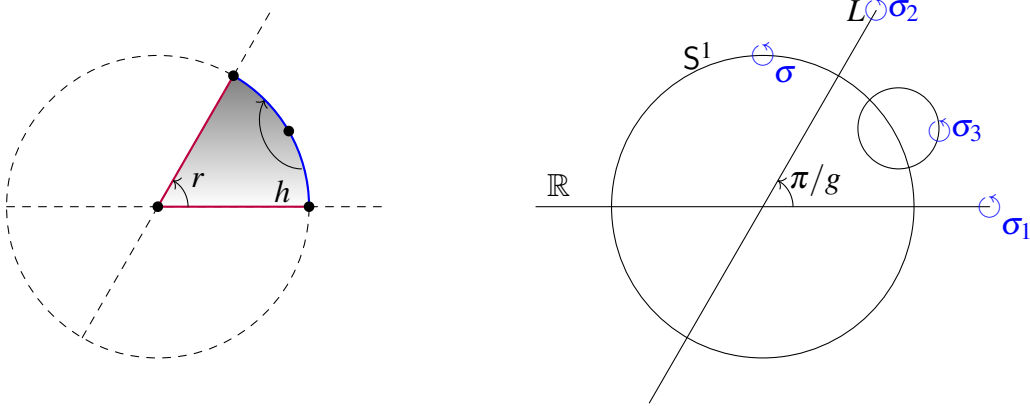


FIGURE 4. On the left is a fundamental domain for the action of the group $D_g = \langle r, h \rangle$. On the right, the transformations f_j are formed by the reflections $\sigma, \sigma_1, \sigma_2, \sigma_3$ defined in Section 3.

Proposition 3.1. *With the notation as above, $\langle r, h \rangle \simeq D_g$, the dihedral group of order $2g$, and also $D_g \subseteq \text{Aut}(G)$. The signature of D_g acting on S is $(0; 2, 2, 2, 2, g)$.*

Proof. One checks readily that a fundamental domain for $\langle r, h \rangle$ is given by the sector of the unit disc cut out by \mathbf{R} and L , in the positive quadrant. One views this as having four arcs as edges, paired by r and h as in Fig. 4. With this we can apply the Poincaré polyhedron theorem (cf. [Mas87, §IV.F.5]) which implies that a presentation for the group $\langle r, h \rangle$ has exactly the same relations as the dihedral group of order $2g$:

Since r and h are Möbius transformations, they will induce an automorphism on S if conjugation by them preserves G . That is, we need to check that $rf_k r^{-1}$ and $hf_k h^{-1}$ lie in G for all k . Indeed, we have $rf_k r^{-1} = r r^k \sigma_1 \sigma_3 r^{-k} r^{-1} = f_{k+1} \in G$, and

$$\begin{aligned} hf_k h^{-1} &= h(r^k \sigma_1 \sigma_3 r^{-k}) h^{-1} \\ &= \sigma \sigma_1 (\sigma_2 \sigma_1)^k \sigma_1 \sigma_3 (\sigma_1 \sigma_2)^k \sigma_1 \sigma \\ &= (\sigma \sigma) (\sigma_1 \sigma_2)^k (\sigma_1 \sigma_1) \sigma_3 \sigma_1 (\sigma_2 \sigma_1)^k \\ &= g^{-k} \sigma_3 \sigma_1 g^k \\ &= \left(r^{g-k} \sigma_1 \sigma_3 r^{-(g-k)} \right)^{-1} \\ &= f_{g-k}^{-1} \in G. \end{aligned}$$

Hence the group $\langle r, h \rangle = D_g$ is a subgroup of $\text{Aut}(S)$. To compute its signature, notice that the orbits under the group action are the images under the quotient map $\Omega(G) \rightarrow S$ of the following points:

- (1) $\{0, \infty\}$
- (2) $e^{2k\pi i/g}$ for $k = 1, \dots, g$
- (3) $e^{(2k+1)k\pi i/2g}$ for $k = 1, \dots, g$
- (4) $e^{2ki\theta/2g}$ for $k = 1, \dots, g$
- (5) $e^{2ki\eta/2g}$ for $k = 1, \dots, g$

This implies the branch points of the quotient $S \rightarrow S/D_g$. To compute the genus g_0 of S/D_g we apply the Riemann–Hurwitz formula:

$$g - 1 = |D_g|(g_0 - 1) + \frac{1}{2} \sum_{i=1}^s \left(1 - \frac{1}{m_i}\right) = 2g(g_0 - 1) + \frac{1}{2}(5 - 2 - \frac{1}{g}) = 2gg_0 + g - 1.$$

This implies that $g_0 = 0$. □

We compute directly the action of the subgroup $D_g = \langle r, h \rangle \leq \text{Aut}(S)$.

Lemma 3.2. *The action of r and h satisfy $r^*\omega_j = \omega_{j+1}$ and $h^*\omega_j = -\omega_{g-j}$.*

Proof. This follows by a direct computation. □

Corollary 3.3. *The map $z \mapsto -z$ acts nontrivially as a reciprocal under ϕ_S in genus 2 in the sense that $\tilde{\phi}_S(-z) \cdot \tilde{\phi}_S(z) = 1$.*

Proof. The rotation matrix acts by $z \mapsto -z$ in the case of genus 2. □

We now show that h is the hyperelliptic involution in the case of $g = 2$.

Proof of Theorem 1.4 Weierstrass points. Notice that $h(z) = 1/z$ has fixed points $1, -1$. Moreover $h(e^{i\psi}) = e^{-i\psi}$ which is identified with $e^{i\psi}$ under identification of circles in genus 2 when $\psi = \theta, \eta, \pi - \theta, \pi - \eta$. We get 6 fixed points, by [FK92, III.7.9] this classifies the Weierstrass points of the hyperelliptic involution (See Fig. 2).

We finish by justifying that we can take the coordinate chart of projective space where $\omega_1(z) \neq 0$, which holds since there are $2g - 2 = 2$ zeroes of any holomorphic differential Theorem 2.3. The zero of $\omega_1(z)$ at $z = \infty$ has order 2 since the denominator of each term contains a z^2 so $\omega_1(z)$ is nonzero in the fundamental domain.

To see that the images of the Weierstrass points come in reciprocal pairs, notice $x_1 = -x_2$, $x_4 = -x_6$, and $x_3 = -x_5$. Combining this fact with Corollary 3.3, we conclude the images are indeed reciprocal values. □

3.1. Non-Hyperelliptic proof. It is left to prove Theorem 1.5.

Lemma 3.4. *The group G is a Fuchsian Schottky group of rank g . Moreover G keeps invariant the unit circle and the fixed points of each f_i all lie on a common circle in the following cycle configuration*

$$(A_1, B_1, A_2, B_2, \dots, A_g, B_g).$$

Where the order to be taking is clockwise, see for example Fig. 2.

Proof. The group G pairs g pairs of circles equally spaced about the unit circle, therefore it is Schottky. Since each f_k is defined as a product of reflections in circles and lines orthogonal to the unit circle, this group is Fuchsian. Since σ commutes with all of σ_1 , σ_2 , and σ_3 , hence each f_k (and therefore the entire group G) preserves the unit circle. Direct inspection shows the last part of the lemma. \square

We will be using the notion of harmonic pairs, as introduced in [Kee80, Definition 1.1a], which we recall here for completeness. For $x, y, u, v \in \mathbf{C}$ on a common line, we denote the cross-ratio as

$$(x, y; u, v) := \frac{u-x}{u-y} \cdot \frac{v-y}{v-x}.$$

Definition 3.5. Let f_i and f_j be Möbius transformations with fixed points (A_i, B_i) and (A_j, B_j) which are distinct. The unique pair of points (u, v) in \mathbf{CP}^1 for which the cross-ratio

$$(A_i, B_i; u, v) = (A_j, B_j; u, v) = -1$$

is called the harmonic pair with respect to f_i and f_j .

Definition 3.6. We say a Schottky group Γ admits a mutually harmonic set of generators if there exists generators f_1, \dots, f_g of Γ and a pair of points (u, v) which are harmonic with respect to f_i and f_j for every i, j .

Lemma 3.7. [Kee80, Lemma 2] Every hyperelliptic Riemann surface is uniformized by a Schottky group with a mutually harmonic set of generators.

Lemma 3.8. If $g \geq 3$, then S is not hyperelliptic.

Proof. Assume S is hyperelliptic. By Lemma 3.7 there exists a Schottky group Γ admitting a mutually harmonic set of generators $\tilde{f}_1, \dots, \tilde{f}_g$ with respect to a pair of points (u, v) . Since Γ and G must be conjugate by some Möbius transformation ϕ , therefore $\tilde{f}_i = \phi^{-1} \circ f_i \circ \phi$ for every $i = 1, \dots, g$.

In particular, if we denote by (A_i, B_i) the fixed points of f_i , then the fixed points of \tilde{f}_i are $(\phi^{-1}(p_i), \phi^{-1}(q_i))$. Since all of the fixed points of each f_i lie in a common circle by Lemma 3.4, all the fixed points of \tilde{f}_i will lie on a common circle. Notice that the only way for $\tilde{f}_1, \dots, \tilde{f}_g$ to be a mutually harmonic set of generators implies that the pair of points must be $(u, v) = (0, \infty)$. The configuration of the fixed points given in Lemma 3.4 cannot be mapped in that way. This gives the desired contradiction and shows that S it is not hyperelliptic. \square

4. EXPLICIT COMPUTATIONS

In this Section we will first analyze the cases of complete intersections, corresponding to genus 3 and 4. We also write out how we compute explicitly the Möbius transforms and circles for the family $S_{\eta, \theta}$.

Let $S := S_{\eta, \theta}$ be a Riemann surface of genus $g > 2$ as given in Definition 1.2, then Theorem 1.5 gives an embedding of S in \mathbf{CP}^{g-1} as an algebraic subvariety. Denote by $I_S \subseteq \mathbf{C}[x_0, \dots, x_{g-1}]$ the ideal of $\phi_S(S)$ and by $(I_S)_d$ its homogeneous component of degree d , this is a

finite dimensional vector space. The group D_g acts linearly on the space $H^0(S, \Omega_S)$ of holomorphic 1-forms. Hence induces an action in the space of monomials of degree d in x_0, \dots, x_{g-1} that preserve $(I_S)_d$.

Lemma 4.1. *The group D_g acts as follows:*

(1) $r(z) = \exp(2\pi i/g)z$: $r^* \omega_j = \omega_{j+1}$, so we get a cyclic action of the canonical curve:

$$[x_0 : \dots : x_{g-1}] \mapsto [x_1 : \dots : x_{g-1} : x_0].$$

(2) $h(z) = 1/z$: $h^* \omega_j = -\omega_{g-j}$, so we get the action

$$[x_0 : x_1 : \dots : x_{g-1}] \mapsto [x_0 : x_{g-1} : \dots : x_1]$$

(i.e. the first coordinate is fixed and the remaining $g-1$ coordinates are reversed; because we use homogeneous coordinates we can ignore the factor of -1 picked up in each coordinate).

Proof. Follows by a direct computation. □

4.1. Genus 3. Let $S \subseteq \mathbf{CP}^2$ be a Riemann surface of genus 3 from Definition 1.2. Lemma 2.5 guarantees the ideal $I_S \subseteq \mathbf{C}[x_0, x_1, x_2]$ is generated by a unique polynomial $F(x_0, x_1, x_2)$ of degree 4. For every $g \in D_3$ we necessarily have that $g^*F = \lambda F$ for some non-zero constant. The orbits of the degree 4 monomials under the action of D_3 are the following:

$$\{x_0^4, x_1^4, x_2^4\}, \{x_0^3x_1, x_0^3x_2, x_0x_1^3, x_0x_2^3, x_1^3x_2, x_1x_2^3\}, \{x_0^2x_1^2, x_1^2x_2^2, x_1^2x_2^2\}, \{x_0^2x_1x_2, x_0x_1^2x_2, x_0x_1x_2^2\}$$

Hence the quartic is of the form

$$\begin{aligned} F(x_0, x_1, x_2) = & c_1(x_0^4 + x_1^4 + x_2^4) + c_2(x_0^3x_1 + x_0^3x_2 + x_0x_1^3 + x_0x_2^3 + x_1^3x_2 + x_1x_2^3) \\ & + c_3(x_0^2x_1^2 + x_1^2x_2^2 + x_1^2x_2^2) + c_4(x_0^2x_1x_2 + x_0x_1^2x_2 + x_0x_1x_2^2). \end{aligned}$$

Remark 4.2. *There exists a unique action up-to projective linear transformations of D_4 on a quartic curve in \mathbf{CP}^2 , cf. [KK79]. Hence the equations are common to all quartics with an action of D_4 . Moreover, there is a change of coordinates that makes $c_2 = 0$. So this construction depends on 2 parameters. Due to the non-uniqueness of this transformation we prefer not to make this change of coordinates.*

Specifically to our case are the real structure and their fixed points, this gives a way of making more precise the equation of such quartic by evaluating on very few points.

Notice that the action of h on \mathbf{CP}^2 has as fixed locus the line $x_1 = x_2$ together with the point $[0 : 1 : -1]$. Intersection the line $x_1 = x_2$ with the curve S gives 4 fixed points on the curve. Representatives of these points in Ω are given by $1, -1, \exp(\theta i), \exp(\eta i)$. Hence we have

$$\begin{aligned} \phi_S(1) &= [1 : u_1 : u_1] & \phi_S(-1) &= [1 : u_2 : u_2] \\ \phi_S(e^{\theta i}) &= [1 : u_3 : u_3] & \phi_S(e^{\eta i}) &= [1 : u_4 : u_4] \end{aligned}$$

$$\phi_S(1) = [1 : u_1 : u_1] \quad \phi_S(-1) = [1 : u_2 : u_2] \quad \phi_S(e^{\theta i}) = [1 : u_3 : u_3] \quad \phi_S(e^{\eta i}) = [1 : u_4 : u_4]$$

We therefore obtain a system of equations in the variables c_1, c_2, c_3, c_4 by evaluating the points above on the equation F .

4.2. **Genus 4.** Let $S \subseteq \mathbf{CP}^3$ be a Riemann surface of genus 4 as in Definition 1.2. Lemma 2.5 says the ideal $I_S \subseteq \mathbf{C}[x_0, x_1, x_2, x_3]$ is generated by two polynomials Q, T of degrees 2 and 3 respectively. The orbits of the degree two monomials under the action of D_4 are

$$\{x_0^2, x_1^2, x_2^2, x_3^2\}, \{x_0x_1, x_1x_2, x_2x_3, x_3x_0\}, \{x_0x_2, x_1x_3\}$$

hence the quadric Q is of the form

$$\begin{aligned} Q(x_0, x_1, x_2, x_3) &= c_1(x_0^2 + x_1^2 + x_2^2 + x_3^2) \\ &\quad + c_2(x_0x_1 + x_1x_2 + x_2x_3 + x_3x_0) \\ &\quad + c_3(x_0x_2 + x_1x_3). \end{aligned}$$

The orbits of the degree three monomials under the cyclic action r^* in item (1) of Lemma 4.1 are

$$\begin{aligned} &\{x_0^3, x_1^3, x_2^3, x_3^3\}, \\ &\{x_0x_1^2, x_1x_2^2, x_2x_3^2, x_3x_0^2\}, \{x_0^2x_1, x_1^2x_2, x_2^2x_3, x_3^2x_0\}, \\ &\{x_0^2x_2, x_1^2x_3, x_2^2x_0, x_3^2x_1\}, \\ &\{x_0x_1x_2, x_1x_2x_3, x_2x_3x_0, x_3x_0x_1\}. \end{aligned}$$

The transformation h^* in item (2) of Lemma 4.1 sends $x_0x_1^2$ to $x_3^2x_0$ and so the two orbits on the second line of the above display are combined into a single orbit; one sees that no other orbits combine (since h^* exactly swaps x_1 and x_3 and fixes x_0 and x_2) so in total we have four orbits and the cubic polynomial T is

$$\begin{aligned} T(x_0, x_1, x_2, x_3) &= d_1(x_0^3 + x_1^3 + x_2^3 + x_3^3) \\ &\quad + d_2(x_0x_1^2 + x_1x_2^2 + x_2x_3^2 + x_3x_0^2 + x_0^2x_1 + x_1^2x_2 + x_2^2x_3 + x_3^2x_0) \\ &\quad + d_3(x_0^2x_2 + x_1^2x_3 + x_2^2x_0 + x_3^2x_1) \\ &\quad + d_4(x_0x_1x_2 + x_1x_2x_3 + x_2x_3x_0 + x_3x_0x_1). \end{aligned}$$

This exhibits $2 + 3 = 5$ parameters (generically we can divide through and assume $c_3 = d_4 = 1$) for the genus 4 curve; we expect $3g - 3 = 9$ parameters for the generic genus 4 curve but of course this one is highly symmetric. From the symmetry in fact we should see only two parameters, the angles θ and η , with the parameters $c_1, c_2, d_1, d_2,$ and d_3 functions of θ and η via the uniformizing map.

By the discussion above, we see that the fixed point locus of h on \mathbf{CP}^3 is the plane $x_1 = x_3$ together with the two points $[0 : 1 : 0 : \pm 1]$. Intersecting the plane with the canonical curve (which is degree 6), we get six fixed points on the curve. These are all the fixed points of h , and the two points $[0 : 1 : 0 : \pm 1]$ do not lie on the canonical curve. The six fixed points are represented in Ω by $1, -1, \exp(\theta i), \exp(\eta i), \exp(\pi i - \theta i),$ and $\exp(\pi i - \eta i)$. We therefore have

$$\begin{aligned} \phi_S(1) &= [1 : u_1 : v_1 : u_1] & \phi_S(-1) &= [1 : u_2 : v_2 : u_2] \\ \phi_S(e^{\theta i}) &= [1 : u_3 : v_3 : u_3] & \phi_S(e^{\pi i - \theta i}) &= [1 : u_4 : v_4 : u_4] \\ \phi_S(e^{\eta i}) &= [1 : u_5 : v_5 : u_5] & \phi_S(e^{\pi i - \eta i}) &= [1 : u_6 : v_6 : u_6] \end{aligned}$$

where the twelve new variables u_k and v_k for $1 \leq k \leq 6$ give six known points on the curve. One can now use algebra to fit the hypersurfaces Q and T onto these six known points (the system is highly over-determined): we obtain a system of seven equations

$$0 = Q(1, u_1, v_1, u_1) = Q(1, u_2, v_2, u_2) = T(1, u_1, v_1, u_1) = T(1, u_2, v_2, u_2) = T(1, u_3, v_3, u_3)$$

in the five variables $c_1, c_2, d_1, d_2,$ and d_3 which can be used to write down the canonical curve based only on evaluating the canonical map at five general points.

4.3. Explicit circles and mappings. In this section we choose a fixed matrix to map between two isometric circles, and compute the fixed points. To map one isometric circle onto another circle, we are able to choose the amount of rotation. We will choose the amount of rotation so that the matrices have positive real trace, which will be in fact strictly larger than 2. This can be seen by using the characterization of the action of Möbius transformations on the complex plane up to conjugation by their fixed points, or equivalently their trace [Mas87, Chapter I]. Specifically given two isometric circles we identify them with the following lemma.

Lemma 4.3. *Consider two disjoint circles in \mathbf{C} centered at z and w with the same radius $r > 0$, $C = S(z, r)$ and $C' = S(w, r)$. Suppose f is defined by*

$$f = \begin{bmatrix} a & b \\ c & d \end{bmatrix} \quad \text{for} \quad a = \frac{w}{r}e^{i\theta} \quad d = -\frac{z}{r}e^{i\theta} \quad c = \frac{1}{r}e^{i\theta} \quad b = \frac{ad-1}{c} = -\frac{wze^{2i\theta} + r^2}{re^{i\theta}}$$

satisfying $f(C) = C'$ and $f(B(z, r)) = \mathbf{C} \setminus B(w, r)$. In order for the trace to be real and positive, we set

$$\theta_0 = -\arg(w - z).$$

The two fixed points are given by the attracting, respectively repelling fixed points A and B where

$$A = \frac{a-d + \sqrt{(a-d)^2 + 4bc}}{2c} \quad B = \frac{a-d - \sqrt{(a-d)^2 + 4bc}}{2c}.$$

Proof of Lemma 4.3. We first show $f(C) = C'$. Let $p \in \mathbf{C}$ so $|p - z| = r$. We compute

$$|f(p) - w| = \left| \frac{\frac{e^{i\theta}}{r}wp - \frac{wze^{2i\theta} + r^2}{re^{i\theta}}}{\frac{e^{i\theta}}{r}p - \frac{z}{r}e^{i\theta}} - w \right| = \left| \frac{e^{2i\theta}w(p-z) - r^2}{e^{2i\theta}(p-z)} - w \right| = r,$$

which is sufficient since f is invertible. Since f preserves the circle, we only need to check one point in the interior. Notice that $f(z) = \infty$, so $f(B(z, r)) = \mathbf{C} \setminus B(w, r)$. The choice of θ_0 guarantees the trace is given by

$$a + d = \frac{e^{i\theta_0}}{r}(w - z) = \frac{1}{r}|z - w| \in \mathbf{R}_{>0}.$$

Finally to compute the fixed points, the fixed points satisfy

$$az + b = z(cz + d) \Leftrightarrow cz^2 + (d - a)z - b = 0,$$

where the solution comes from the quadratic formula and the fact that circles are disjoint implies the discriminant is nonzero. \square

Proposition 4.4. *For the real curves $C_i = C(z_i, r)$ to $C'_i = C(w_i, r)$ given in Definition 1.2 we have the following formulas:*

$$z_1 = \exp\left(i\frac{\theta + \eta}{2}\right) \sec\left(\frac{\theta - \eta}{2}\right) \quad r = \tan\left(\frac{\theta - \eta}{2}\right),$$

and for $j = 2, \dots, g$

$$w_1 = \bar{z}_1 \quad z_j = e^{\frac{2\pi i}{g}(j-1)} z_1 \quad w_j = e^{\frac{2\pi i}{g}(j-1)} w_1.$$

Proof. We first notice that the four circles are all orthogonal to the unit circle, so reflection across the unit circle provides a real structure for the curve.

Next we will focus on constructing the center and radius of C_1 . Recall C_1 is the circle orthogonal to the unit circle S^1 which goes through the points $e^{i\eta}$ and $e^{i\theta}$. In order to find the Euclidean center, we take the intersection point of the tangent lines to the unit circle at $e^{i\theta}$ and $e^{i\eta}$, respectively. The tangent lines are given by finding the lines orthogonal to the radial line through $e^{i\theta}$ and $e^{i\eta}$

$$y - \sin(\eta) = -\frac{\cos(\eta)}{\sin(\eta)}(x - \cos(\eta)) \quad y - \sin(\theta) = -\frac{\cos(\theta)}{\sin(\theta)}(x - \cos(\theta)).$$

So the center of the circle is given by

$$z_1 = \cos\left(\frac{\theta + \eta}{2}\right) \sec\left(\frac{\theta - \eta}{2}\right) + i \sin\left(\frac{\theta + \eta}{2}\right) \sec\left(\frac{\theta - \eta}{2}\right)$$

with radius found by taking the distance from z_1 to $e^{i\eta}$:

$$r_1 = \sqrt{(\cos(\eta) - \Re(z_1))^2 + (\sin(\eta) - \Im(z_1))^2} = \tan\left(\frac{\theta - \eta}{2}\right).$$

Since all the circles have the same radius, we have now found the correct radius for the six circles. The other centers are given by applying the correct complex conjugation to get w_1 , and then rotating by $2\pi/g$. The fact that we get a Schottky group and thus a Riemann surface comes from Proposition 2.7. \square

5. NUMERICAL EXPERIMENTS

In this section we first share information about the algorithm and code used for making the experiments. We next include computations for genus 2 where we give approximate Weierstrass points and then in genus 3 where we approximate the quartic defining the curve by looking at the real points.

5.1. An algorithm for generating elements of the free group. Algorithm 5.1 inputs pairs of isometric circles and outputs the elements in the Schottky group up to level L . This algorithm minimizes the amount of matrix multiplication needed in order to store elements of the Schottky group. The key idea is when generating a word, we also add a “tag” which keeps track of what generator is on the right side of the word. This idea of keeping track of the tags was given in [MSW02, p.115] and this algorithm is the same but easier to read since it uses capabilities of modern programming languages. Keeping track of the tags is also the key idea to detecting elements of the coset representatives G/G_n , so the remaining implementation for evaluating

the Poincare series at points on the Riemann surface is elementary. See [Mat24] for an implementation in Julia [BEKS17], which is how the following computations were generated.

Algorithm 5.1 From circles to words in Schottky groups

```

1: Input  $g$  centers  $z_1, \dots, z_g$ 
2: Input  $g$  centers  $w_1, \dots, w_g$ 
3: Input  $g$  radii  $r_1, \dots, r_g > 0$ 
4: Input length of words generated  $L$ .
5: for  $i = 1, \dots, g$  do
6:    $f_i = \begin{bmatrix} \frac{w_i}{r_i} & -\frac{w_i z_i}{r_i} - r_i \\ \frac{1}{r_i} & \frac{-z_i}{r_i} \end{bmatrix}$  ▷ as in Lemma 4.3
7: end for
8: procedure MATRIXWORDS( $g, L$ ) ▷ Construct words in Schottky group of length  $\leq L$ 
9:    $list = [(Id_2, 0)]$  ▷  $Id_2$  is  $2 \times 2$  identity matrix, tag is 0
10:  for  $level = 1, \dots, L$  do
11:     $oldlist \leftarrow list$  ▷  $oldlist$  has all words length  $< level$ 
12:    for  $w \in oldlist$  do
13:      if  $w[2] \neq -j$  then add  $(w[1] \cdot f_j, j)$  to  $list$ 
14:      end if
15:      if  $w[2] \neq j$  then add  $(w[1] \cdot f_j^{-1}, -j)$  to  $list$ 
16:      end if
17:    end for
18:  end for
19:  return  $[w[1]$  for  $w$  in  $list]$ 
20: end procedure

```

5.2. Numerical Weierstrass Points Genus 2. We consider $\eta = \frac{\pi}{12}$ and $\theta = \frac{\pi}{4}$ which were used to sketch Fig. 2. We estimate the equation of the curve is

$$y^2 = \prod_{j=1}^6 (x - \alpha_j)$$

where $\alpha_j \approx \tilde{\phi}_S(x_j)$ calculated for words of length $L \leq 12$. The values are approximated as follows, where the imaginary components are dropped as they all appear on the order of 10^{-11}

$$\begin{aligned} \alpha_1 &= -11.47448708745693 & \alpha_3 &= 4.084600885787089 & \alpha_4 &= -11.787692546430492 \\ \alpha_2 &= -0.08714986494625039 & \alpha_5 &= 0.2448219613030484 & \alpha_6 &= -0.08483424521467196 \end{aligned}$$

We notice that the real structure can be seen here as all of the imaginary components of the roots are zero. We also verify the reciprocal values of the roots are given by

$$\alpha_1 \alpha_2 = 0.9999999999993655, \quad \alpha_3 \alpha_5 = 0.9999999999985639, \quad \alpha_4 \alpha_6 = 0.999999999990453.$$

Finally, we plot the curve for real values of x and y in Fig. 5.

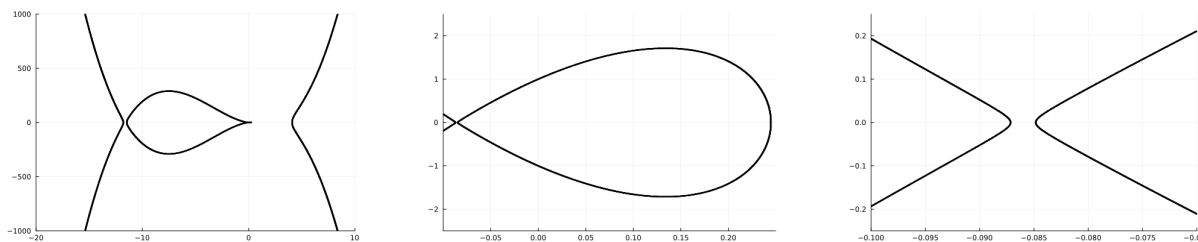


FIGURE 5. A representation of the real points of the genus 2 curve with $\eta = \frac{\pi}{12}$ and $\theta = \frac{\pi}{4}$ on the left. In the middle we zoom in near $x = 0$, and on the right, we zoom further in near $x = -.09$ to see these curves create 3 separate smooth curves.

5.3. Approximating the quartic in genus three. To experiment with genus 3, we decided to sample along the real points of the M -curve, and approximate the quartic to fit the real data. That is we did the following.

- (1) Fix $0 < \eta < \theta < \frac{\pi}{3}$ and choose $N, L \geq 1$.
- (2) Sample N points uniformly on the unit circle and compute the approximate image in \mathbf{CP}^2 by truncating the Poincaré theta series of Proposition 1.1 to words of length at most L .
- (3) Plot the real points in the plane by taking the chart in \mathbf{CP}^2 where the third component is 1. We also truncate to the real parts since the imaginary parts are small. This is used to form the scatter plots in Fig. 6 and Fig. 7.
- (4) Now we add a contour plot of the level sets by plotting the real part of our approximate polynomial $p(z_1, z_2, z_3)$ at $p(x, y, 1)$. To obtain the approximate polynomial, we solve a homogeneous least squares problems $Ax = 0$ subject to the constraint $\|x\| = 1$, where x is a basis of monomials, and A is the $N \times 15$ matrix formed by evaluating the monomials at the N sample points.

Example 5.1. Consider $\eta = \pi/12$, $\theta = \pi/4$, $N = 50$ and $L = 8$. We obtained the following equation, where the imaginary parts are on the order of 10^{-8} and we keep only the first 6 decimal places

$$\begin{aligned}
p(z_1, z_2, z_3) = & -0.006341z_1^4 - 0.006347z_2^4 - 0.006352z_3^4 - 0.039327z_1^3z_2 - 0.039291z_1^3z_3 \\
& - 0.039302z_1z_2^3 - 0.298144z_1^2z_3^2 - 0.039225z_2z_3^3 - 0.039441z_1z_3^3 \\
& - 0.298246z_1^2z_2^2 - 0.298398z_2^2z_3^2 - 0.039336z_2^3z_3 \\
& + 0.490895z_1^2z_2z_3 + 0.491323z_1z_2^2z_3 + 0.491268z_1z_2z_3^2.
\end{aligned}$$

Notice that the Equation closely follows the symmetry of the curve expected from Section 4.1 by only sampling 50 points and truncating the series after words of length 8. In Section 6.1 we discuss potential options and difficulties for obtaining better estimates.

See also Fig. 6 for a plot of the sampled points and a contour plot of the approximate polynomial.

We remark that (3) could generate issues as the Poincare theta series do not converge at the fixed points A_n, B_n which live on the unit circle. Naturally we can first just hope this doesn't

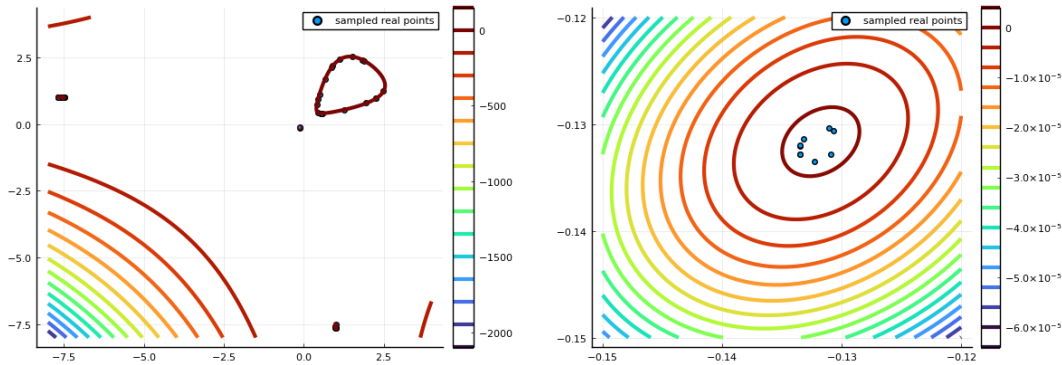


FIGURE 6. From Example 5.1 we plot uniformly sampled real points in blue alongside a contour plot of the approximate polynomial. Notice that there is red at each of the 3 dots, as well as the one loop we can see which correspond to the 4 ovals making this an M -curve. On the right we zoom in very close to $(0,0)$, where the quartic in fact detects this very small oval as well.

happen since they form a set of measure zero when sampling on the unit circle. Alternatively to guarantee convergence, one could sample uniformly on each of the intervals of the unit circle which are exterior to the circles. By doing this it is also nice to see from Fig. 2 that the small intervals between C_j and C'_j form the smaller 3 circles in Fig. 6, whereas the three intervals between C_1, C'_2 and C_2, C'_3 and C_3, C'_1 combine to form the one larger oval.

Next we remark that in (4) the least squares solution to the homogeneous solution of equations (see [Ink05]) requires taking the eigenvector associated to the smallest eigenvalue of $A^T A$ up to a normalization. However in our experiments our smallest eigenvalue was numerically 0, so instead we could just project onto the null space by computing $(I_{15} - A^+ A) \vec{1}$ where A^+ is the Moore–Penrose pseudoinverse, and $\vec{1}$ is the vector of all 1s. Note $I_{15} - A^+ A$ is the orthogonal projection onto the null space, so the choice of $\vec{1}$ is arbitrary and we can just normalize the vector to norm 1.

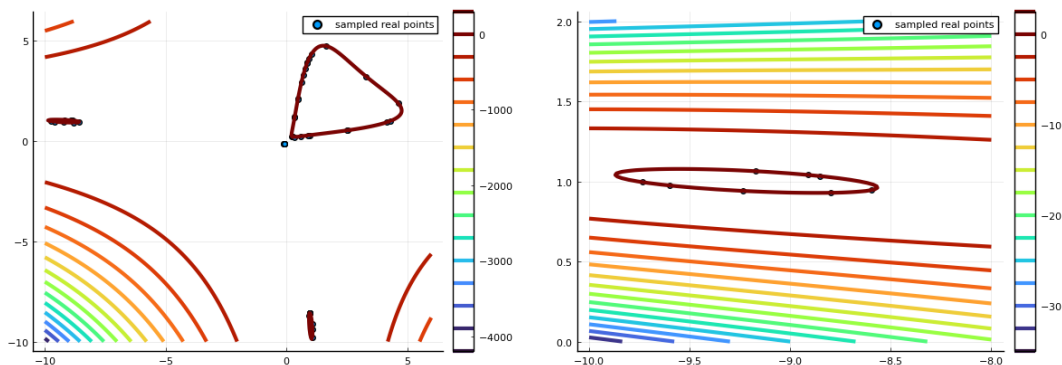


FIGURE 7. In this case we consider $\eta = \pi/9$ and $\theta = 2\pi/9$ $N = 50$ and $L = 8$, in order to see a more symmetric situation in the real ovals. The blue points are sampled uniformly along the unit circle, and the contour map overlaid represents the polynomial approximation. On the right image we zoom into the far left oval to see the approximation polynomial matches very well to the given real points.

Notice that we need $N \geq 15$ in order to have enough sample points on the curve, but we chose $N = 50$ since it was small enough to regularly show all four ovals while still leaving very short computational times of at most 1 minute. We expect we would obtain much more accurate information using more refined methods of learning varieties from curves [BKS^W18]. The remarkable part here is that our simple method with a low level of accuracy allows us to find a quartic that can see all 4 ovals.

5.4. Computing the Riemann Matrix. In this section, we want to use the following theorem to approximate the Riemann Matrix for $g = 3$. To do this, for each $n = 1, \dots, g$, define μ_n so that

$$\frac{f_n(z) - A_n}{f_n(z) - B_n} = \mu_n \frac{z - A_n}{z - B_n}, \quad |\mu_n| < 1,$$

in which case A_n is the attracting and B_n the repelling fixed point. Namely if f is our fixed transformation from Lemma 4.3, the associated value of μ is given by

$$\mu = \frac{a - Ac}{a - Bc}$$

We fix a basis of homology a_j, b_j by setting a_j to follow the boundary of C_j counterclockwise, and b_j to be the closed loop connecting C_j to C'_j .

Theorem 5.2. [BBE⁺94, Theorem 5.1] *The Riemann matrix normalized to this basis of differentials is given by*

$$R_{nm} = \frac{1}{2\pi i} \begin{cases} \sum_{f \in G_m \setminus G/G_n} \log\{A_m, B_m, fA_n, fB_n\} & m \neq n \\ \log \mu_n + \sum_{f \in G_m \setminus G/G_n, f \neq I} \log\{A_m, B_m, fA_n, fB_n\} & m = n \end{cases} \quad (5.1)$$

where the curly brackets are the cross-ratio

$$\{z_1, z_2, z_3, z_4\} = (z_1 - z_3)(z_2 - z_4)(z_1 - z_4)^{-1}(z_2 - z_3)^{-1}.$$

We refer the reader to [Sch11] for further discussion on computing rates of convergence. For our purposes we wanted to see the fact that we indeed have M -curves by having a purely imaginary Riemann matrix. Indeed for $\eta = \pi/12$ and $\theta = \pi/4$ generating words of length at most 10, we approximated the Riemann matrix of the genus 3 curve by

$$i \begin{bmatrix} 0.39980895499614727 & -0.004497125148067202 & -0.004497125148229181 \\ -0.004497125148067202 & 0.3998089549956627 & -0.004497125149408407 \\ -0.004497125148229181 & -0.004497125149408407 & 0.3998089549963685 \end{bmatrix},$$

where the real part was on the order of 10^{-12} . To obtain the decimal point accuracy for this computation we refer the reader to Section 6.1 and [Sch11, Lemma 4.3.3].

6. FINAL DISCUSSION

In this paper we have focused on the description of algebraic curves for small genus. Our framework however is more general and works in any genus. In particular [BKS^W18] provides a source for general strategies to recover algebraic curves from point sets. We also conclude with a few words on quantifying convergence, other families of curves, and moduli.

6.1. Quantifying convergence. In order to obtain estimates on numerical accuracy we know of two methods: one away from compact sets and the other for different truncation options.

In the first case, we quantify the remainder by considering the summation of the Poincaré theta series truncated by word length of f with $|f|$. The next Lemma is essentially proven in [Bog12, Lemma 6.1], which only deals with hyperelliptic curves, but in fact works for any Fuchsian Schottky groups by applying the transformation T mapping the unit circle to the real line.

Lemma 6.1. (*Bogatyrev*) *We have*

$$\sum_{|f|>k, f \in G/G_n} \left| \frac{1}{z-f(B_n)} - \frac{1}{z-f(A_n)} \right| \leq \left[\frac{1}{\text{dist}(\mathbf{K}, \Lambda(G))^2} + o(1) \right] (\sqrt{\mathbf{q}} + 1) \left(\frac{\sqrt{\mathbf{q}} - 1}{\sqrt{\mathbf{q}} + 1} \right)^k$$

where $z \in \mathbf{K}$ is a compact subset of $\Omega(G)$ and $o(1) \rightarrow 0$ as $k \rightarrow \infty$ and \mathbf{q} is a function of θ and η and g , and can be made explicit in terms of cross-ratios of specific points on the circle.

Proof. The proof of [Bog12, Lemma 6.1] applies line by line, since with the Möbius transformation T our circles are all orthogonal to the real line. Möbius transformations preserve cross-ratios, hence the estimates in loc.cit. are the same. \square

Now the key idea is that once we fix η, θ , the rate of convergence is a function of the distance of our sample points from the real line. Though we might apriori be missing key geometries of the curve by sampling so far away from the limit set, but since the structure is algebraic, knowing even a little bit of the curve should give us all the information we need. To obtain explicit numerical information, the $o(1)$ quantity must be made explicit.

In the second case, we refer the reader to [Sch11], but provide a specific case for comparison. In this case instead of truncating series via word length, the author allows for a more general truncation option via any subset S of G/G_n which is *suffix closed*, which captures the idea that $\tilde{f} \cdot f \in S$ should also have $f \in S$, but for convenience we will present the idea of convergence for S to be all words in G/G_n of length less than k , and set F to be a fixed fundamental domain of S in \mathbf{C} . Set $|\gamma_f|$ to be the modulus of the bottom left entry the 2×2 matrix representing f , which controls the radius of the isometric circles. We will consider a function κ_k for $k \in \mathbf{N}$ which is very close to $\min_{\sigma \in G, |\sigma|=k} \left| \frac{\gamma_\sigma}{\gamma_{\hat{\sigma}}} \right|$ ([Sch11, Lemma 4.2.8]), where $\hat{\sigma}$ is the word of length $k-1$ formed by removing the right-most generator in the word. This captures the successive ratios of the circle radii when applying generators. If there is some k large enough so that $2g-1 < \kappa_k^{-2}$ then there is guaranteed convergence of the series [Sch11, Theorem 4.2.10].

We are now prepared to quantify convergence.

Lemma 6.2 (Lemma 4.3.4 [Sch11]). *Fix $k \geq 1$. For k large enough*

$$\left| \sum_{|f|>k, f \in G/G_n} \frac{1}{z-f(B_n)} - \frac{1}{z-f(A_n)} \right| < \left(\min_{\sigma \in G, |\sigma|=k} \min_{z \in F} |z - \sigma(z)| \right)^{-2} \cdot \left(\frac{(1 - \kappa_k^{-2})|A_n - B_n|}{(1 + \kappa_k^{-2})(1 - (2g-1)\kappa_k^{-2})} \right) \sum_{|f|=k} \frac{|\gamma_f|^{-2}}{\min_{z \in F} |A_n - f^{-1}(z)| \cdot \min_{z \in F} |B_n - f^{-1}(z)|}.$$

We remark that the benefit of this lemma is the lack of the $o(1)$ term that needs quantified. However unlike the first case where the cross ratios are simple to compute, in this case we need to compute minimum distances to the fundamental domain over many points, which is computationally expensive to do explicitly. Moreover, here we can see the benefit of choosing different subsets of S instead of taking all words of length up to k as for large k this is a very large set we need to sum over in the computation of the error term as well as κ_k . For more discussion on computation see [Sch11, Section 4.4].

In conclusion there do seem to be some methods for computing error terms, but they are quite involved and require additional computational tools beyond the goal of this paper.

6.2. Other families. We provide some references that would allow the interested reader to consider examples beyond the family of curves presented in Definition 1.2. First, if the reader is interested in M -curves, then the Poincare theta series always converge and the Schottky group is Fuchsian, and the family of such curves can be parametrized [BK11, Section 1.8.3]. In general, we can construct an open subset in \mathbf{C}^{3n} where all of the matrices satisfy the Schottky condition [BK11, Theorem 31], which provides a sufficient condition for absolute convergence of the Poincare theta series. The following family give examples where we have circles sufficiently far apart to guarantee convergence.

Example 6.3. Fix $g \geq 2$. For each $i = 1, \dots, g$ define transformations $f_i = \begin{bmatrix} a_i & b_i \\ c_i & d_i \end{bmatrix}$ with the following conditions.

(1) For all $1 \leq i < j \leq g$, to ensure the isometric circles of f_i and f_j are disjoint:

$$\min \left\{ \left| \frac{a_i}{c_i} - \frac{a_j}{c_j} \right|, \left| \frac{a_i}{c_i} + \frac{d_j}{c_j} \right|, \left| \frac{d_i}{c_i} - \frac{d_j}{c_j} \right| \right\} > \frac{1}{|c_i|} + \frac{1}{|c_j|}$$

(2) For all $1 \leq i \leq g$, to ensure that the two isometric circles of C_i, C'_i are disjoint:

$$\left| \frac{a_i}{c_i} + \frac{d_i}{c_i} \right| > \frac{2}{|c_i|} \iff |a_i + d_i| > 2.$$

From (2) we get loxodromicity of the generators for free and only the $3 \binom{n}{2} + n = \frac{1}{2}(3n^2 - n)$ conditions listed need to be satisfied for the group to be Schottky.

6.3. A few words about moduli. A (not necessarily classical) Schottky group can be characterized as a discrete subgroup of $\mathrm{PSL}_2(\mathbf{C})$ freely generated by purely loxodromic elements [Mas67]. It is known that there exists non-classical Schottky groups, see [Mar74] and references therein.

Following [Ber75] we define the the Schottky space, denoted by \mathcal{S}_g , as the space of sets of g elements in $\mathrm{PSL}_2(\mathbf{C})$ that generate a Schottky group up to Möbius transformations. In order to define a holomorphic structure on \mathcal{S}_g , it can be proved that \mathcal{S}_g is the quotient of the Teichmüller space \mathcal{T}_g by a (not normal) subgroup. Fix G a Schottky group; then locally around G the space \mathcal{S}_g parametrizes holomorphic deformations of the coefficients of generators of G : a choice of generators for G is an element $Z_0 \in (\mathrm{PSL}(2, \mathbf{C}))^g$, and a holomorphic deformation of Z_0 is a holomorphic map $\mu : \Delta \rightarrow (\mathrm{PSL}(2, \mathbf{C}))^g$ such that $\mu(0) = Z_0$. Recall the following.

Theorem 6.4. *Every algebraic curve C of genus $g > 1$ is uniformized by a Schottky group of rank g , and these Schottky groups lie in an open set $U \subseteq \mathcal{S}_g$ with natural coordinates (entries of matrices generating the group) which is locally the neighbourhood of that curve C in \mathcal{M}_g .*

Thus one advantage of studying Schottky groups as models for algebraic curves is the ease of construction: one can immediately write down curves of arbitrary genus (at least numerically, as we studied in earlier sections of this paper) which is a very hard thing to do with purely algebraic machinery [HM98, §6F].

We should point out however that the matrix entries do not provide a nice coordinate system in any geometric sense: they are very local and do not represent any geometric quantities: one natural choice of coordinates are the Fenchel–Nielsen coordinates, which can be generalised to the Kleinian group setting, but the relationship between these coordinates and the matrices generating the uniformizing groups are very subtle.

A promising research direction comes from the theory of compactifications of moduli spaces. The extended Schottky space (cf. [GH88]) parametrizes mild degenerations of Riemann surfaces. This in turn correspond to stable curves, in the sense of Deligne–Mumford. An interesting question will be to find the correct degeneration of our Schottky groups, which correspond to degenerations of the configurations of circles on the plane, to get some canonical embedded stable curves, for which the ideal might be easier to compute.

From the theoretical point of view there are several follow-up questions related with the family introduced in Definition 1.2. A natural question is the field of definition of our family in Definition 1.2. For example, we do not know if for η, θ rational, the corresponding algebraic curve $S_{\eta, \theta}$ in CP^{g-1} will be defined over \mathbf{Q} . Lastly we mention that our family defines a map $\psi : U \rightarrow \mathcal{M}_g$ depending on two real parameters η, θ . Hence makes sense to study its regularity. Although continuity of ψ is immediate, we do not know if, for example, ψ is differentiable.

REFERENCES

- [AC21] Daniele Agostini and Lynn Chua. Computing theta functions with Julia. *J. Softw. Algebra Geom.*, 11:41–51, 2021.
- [ACG11] Enrico Arbarello, Maurizio Cornalba, and Phillip A. Griffiths. *Geometry of algebraic curves. Volume II. With a contribution by Joseph Daniel Harris*, volume 268 of *Grundlehren Math. Wiss.* Berlin: Springer, 2011.
- [AG22] Simonetta Abenda and Petr G. Grinevich. Real regular KP divisors on M-curves and totally non-negative Grassmannians. *Lett. Math. Phys.*, 112(6):64, 2022. Id/No 115.
- [BBE⁺94] E. D. Belokolos, A. I. Bobenko, V. Z. Enol’skij, A. R. Its, and V. B. Matveev. *Algebro-geometric approach to nonlinear integrable equations*. Berlin: Springer-Verlag, 1994.
- [BEKS17] Jeff Bezanson, Alan Edelman, Stefan Karpinski, and Viral B Shah. Julia: A fresh approach to numerical computing. *SIAM review*, 59(1):65–98, 2017.
- [Ber75] Lipman Bers. Automorphic forms for Schottky groups. *Advances in Math.*, 16:332–361, 1975.
- [BHQ18] Eslam Badr, Rubén A. Hidalgo, and Saúl Quispe. Riemann surfaces defined over the reals. *Archiv der Mathematik*, 110(4):351–362, 2018.
- [BK11] Alexander I. Bobenko and Christian Klein, editors. *Computational approach to Riemann surfaces.*, volume 2013 of *Lect. Notes Math.* Berlin: Springer, 2011.
- [BKSW18] Paul Breiding, Sara Kališnik, Bernd Sturmfels, and Madeleine Weinstein. Learning algebraic varieties from samples. *Rev. Mat. Complut.*, 31(3):545–593, 2018.

- [Bob88] Alexander Bobenko. Schottky uniformization and finite-gap integration. *Soviet Math. Dokl.*, 36(1):38–42, 1988.
- [Bog12] Andrei Bogatyrev. *Extremal polynomials and Riemann surfaces. Translated from Russian by Nikolai Kruzhilin*. Springer Monogr. Math. Berlin: Springer, 2012.
- [ÇFM22] Türkü Özlüm Çelik, Samantha Fairchild, and Yelena Mandelshtam. Crossing the transcendental divide: from translation surfaces to algebraic curves, 2022.
- [DHB⁺04] Bernard Deconinck, Matthias Heil, Alexander Bobenko, Mark van Hoeij, and Marcus Schmies. Computing Riemann theta functions. *Math. Comput.*, 73(247):1417–1442, 2004.
- [FK92] Hershel M. Farkas and Irwin Kra. *Riemann surfaces*. Number 72 in Graduate Texts in Mathematics. Springer, 2 edition, 1992.
- [GH78] Phillip Griffiths and Joseph Harris. *Principles of algebraic geometry*. Pure and Applied Mathematics. Wiley-Interscience [John Wiley & Sons], New York, 1978.
- [GH88] L. Gerritzen and F. Herrlich. The extended Schottky space. *J. Reine Angew. Math.*, 389:190–208, 1988.
- [GK05] Jane Gilman and Linda Keen. The geometry of two generator groups: hyperelliptic handlebodies. *Geom. Dedicata*, 110:159–190, 2005.
- [GvdP80] Lothar Gerritzen and Marius van der Put. *Schottky groups and Mumford curves*, volume 817 of *Lect. Notes Math*. Springer, Cham, 1980.
- [HF05] Rubén A. Hidalgo and Jaime Figueroa. Numerical Schottky uniformizations. *Geom. Dedicata*, 111:125–157, 2005.
- [Hid02] Rubén A. Hidalgo. Real surfaces, Riemann matrices and algebraic curves. In *Complex manifolds and hyperbolic geometry (Guanajuato, 2001)*, volume 311 of *Contemp. Math.*, pages 277–299. Amer. Math. Soc., Providence, RI, 2002.
- [Hid05a] Rubén A. Hidalgo. Automorphism groups of Schottky type. *Ann. Acad. Sci. Fenn. Math.*, 30(1):183–204, 2005.
- [Hid05b] Rubén A. Hidalgo. Real schottky parametrizations. *Complex Variables, Theory and Application: An International Journal*, 50(6):401–426, 2005.
- [Hid24] Ruben A. Hidalgo. Computing the field of moduli of some non-hyperelliptic pseudo-real curves, 2024.
- [HM98] Joe Harris and Ian Morrison. *Moduli of curves*, volume 187 of *Grad. Texts Math*. New York, NY: Springer, 1998.
- [Ink05] Keijo Inkilä. Homogenous least squares problem. *Photogrammetric Journal of Finland*, 19(2):34–42, 2005.
- [JW16] Gareth A. Jones and Jürgen Wolfart. *Dessins d’enfants on Riemann surfaces*. Springer Monogr. Math. Cham: Springer, 2016.
- [Kee80] Linda Keen. On hyperelliptic Schottky groups. *Ann. Acad. Sci. Fenn., Ser. A I, Math.*, 5:165–174, 1980.
- [KK79] Akikazu Kuribayashi and Kaname Komiya. On Weierstrass points and automorphisms of curves of genus three. In *Algebraic geometry (Proc. Summer Meeting, Univ. Copenhagen, Copenhagen, 1978)*, volume 732 of *Lecture Notes in Math.*, pages 253–299. Springer, Berlin, 1979.
- [KS22] Mario Kummer and Rainer Sinn. Hyperbolic secant varieties of M -curves. *J. Reine Angew. Math.*, 787:125–162, 2022.
- [Lya22] S. Yu. Lyamaev. On approximate summation of Poincaré series in the Schottky model. *Dokl. Math.*, 106(1):247–250, 2022.
- [Mar74] Albert Marden. Schottky groups and circles. In *Contributions to analysis (a collection of papers dedicated to Lipman Bers)*, pages 273–278. Academic Press, New York-London, 1974.
- [Mar16] Albert Marden. *Hyperbolic manifolds*. Cambridge University Press, 2 edition, 2016. First edition was published under the title “Outer circles”.

- [Mas67] Bernard Maskit. A characterization of Schottky groups. *J. Analyse Math.*, 19:227–230, 1967.
- [Mas87] Bernard Maskit. *Kleinian groups*. Number 287 in Grundlehren der mathematischen Wissenschaften. Springer-Verlag, 1987.
- [Mat24] MathRepo. Mathematical research data repository. *Max Planck Institute for Mathematics in the Sciences*, <https://mathrepo.mis.mpg.de/Schottky2Curves/index.html>, 2024.
- [MSW02] David Mumford, Caroline Series, and David Wright. *Indra’s pearls*. Cambridge University Press, 2002.
- [Mum72] David Mumford. An analytic construction of degenerating curves over complete local rings. *Compositio Math.*, 24:129–174, 1972.
- [Poi85] Henri Poincaré. *Papers on Fuchsian functions*. Springer, 1985.
- [PT21a] Jérôme Poineau and Daniele Turchetti. Berkovich curves and Schottky uniformization I: the Berkovich affine line. In *Arithmetic and geometry over local fields—VIASM 2018*, volume 2275 of *Lecture Notes in Math.*, pages 179–223. Springer, Cham, [2021] ©2021.
- [PT21b] Jérôme Poineau and Daniele Turchetti. Berkovich curves and Schottky uniformization II: analytic uniformization of Mumford curves. In *Arithmetic and geometry over local fields—VIASM 2018*, volume 2275 of *Lecture Notes in Math.*, pages 225–279. Springer, Cham, [2021] ©2021.
- [PT22] Jérôme Poineau and Daniele Turchetti. Schottky spaces and universal Mumford curves over \mathbb{Z} . *Selecta Math. (N.S.)*, 28(4):Paper No. 79, 53, 2022.
- [Rat06] John G. Ratcliffe. *Foundations of hyperbolic manifolds*, volume 149 of *Grad. Texts Math.* New York, NY: Springer, 2nd ed. edition, 2006.
- [Sch11] Markus Schmies. *Computing Poincaré Theta Series for Schottky Groups*, pages 165–182. Springer Berlin Heidelberg, Berlin, Heidelberg, 2011.
- [SD16] Christopher Swierczewski and Bernard Deconinck. Computing Riemann theta functions in Sage with applications. *Math. Comput. Simul.*, 127:263–272, 2016.